

CTGF Loaded Electrospun Dual Porous Core-Shell Membrane For Diabetic Wound Healing

This article was published in the following Dove Press journal:
International Journal of Nanomedicine

Robin Augustine^{1,2}
Alap Ali Zahid^{1,2}
Anwarul Hasan^{1,2}
Mian Wang³
Thomas J Webster³

¹Department of Mechanical and Industrial Engineering, College of Engineering, Qatar University, Doha, Qatar;

²Biomedical Research Center, Qatar University, Doha, Qatar; ³Department of Chemical Engineering, 313 Snell Engineering Center, Northeastern University, Boston, MA 02115, USA

Purpose: Impairment of wound healing is a major issue in type-2 diabetes that often causes chronic infections, eventually leading to limb and/or organ amputation. Connective tissue growth factor (CTGF) is a signaling molecule with several roles in tissue repair and regeneration including promoting cell adhesion, cell migration, cell proliferation and angiogenesis. Incorporation of CTGF in a biodegradable core-shell fiber to facilitate its sustained release is a novel approach to promote angiogenesis, cell migration and facilitate wound healing. In this paper, we report the development of CTGF encapsulated electrospun dual porous PLA-PVA core-shell fiber based membranes for diabetic wound healing applications.

Methods: The membranes were fabricated by a core-shell electrospinning technique. CTGF was entrapped within the PVA core which was coated by a thin layer of PLA. The developed membranes were characterized by techniques such as Scanning Electron Microscopy (SEM), Fourier Transform Infrared Spectroscopy (FTIR) and X-Ray Diffraction (XRD) analysis. In vitro cell culture studies using fibroblasts, keratinocytes and endothelial cells were performed to understand the effect of CTGF loaded membranes on cell proliferation, cell viability and cell migration. A chicken chorioallantoic membrane (CAM) assay was performed to determine the angiogenic potential of the membranes.

Results: Results showed that the developed membranes were highly porous in morphology with secondary pore formation on the surface of individual fibers. In vitro cell culture studies demonstrated that CTGF loaded core-shell membranes improved cell viability, cell proliferation and cell migration. A sustained release of CTGF from the core-shell fibers was observed for an extended time period. Moreover, the CAM assay showed that core-shell membranes incorporated with CTGF can enhance angiogenesis.

Conclusion: Owing to the excellent cell proliferation, migration and angiogenic potential of CTGF loaded core-shell PLA-PVA fibrous membranes, they can be used as an excellent wound dressing membrane for treating diabetic wounds and other chronic ulcers.

Keywords: diabetic wound, CTGF, electrospinning, PVA, PLA

Introduction

Diabetes mellitus is a devastating disease with more than 400 million people affected globally.¹ Chronic ulcers with deep tissue damage in patients with diabetes leads to a high rate of amputation and mortality. Diabetic wounds typically show delayed healing, persistent inflammation, abnormally high exudate production and high bacterial load.² Impaired diabetic wound healing is associated with multiple factors including but not limited to abnormal fibroblast and keratinocyte proliferation, reduced cell migration and decreased angiogenesis.³ These complications ultimately lead to impairment of vascularization, delayed wound contraction and subsequent formation of non-healing diabetic wounds.

Correspondence: Anwarul Hasan
Tel +97470569169
Email hasan.anwarul.mit@gmail.com

Thomas J Webster
Tel +16173736585
Email th.webster@neu.edu

During the past few decades, various biomolecules such as vascular endothelial growth factor (VEGF),⁴ epidermal growth factor (EGF),⁵ platelet derived growth factor (PDGF)⁶ and connective tissue growth factor (CTGF)⁷ have been tried as suitable treatment regimens for managing diabetic wounds.⁸ For instance, CTGF can play an important role in promoting cell proliferation, cell migration and angiogenesis which will improve diabetic wound healing.^{9–11} An earlier study demonstrated that recombinant CTGF stimulates collagen and fibronectin synthesis in cells,¹² and CTGF also promotes the proliferation, migration and differentiation of endothelial cells which are essential for angiogenesis in the wound.¹³ However, the successful clinical application of CTGF in diabetic wounds is limited due to the lack of required bioactivity in the highly oxidative wound environment which necessitates controlled delivery to the wound.¹⁴

In order to minimize complications associated with diabetic wounds, appropriate wound coverage matrices with microbial barrier properties, exudate uptake capacity and wound healing properties should be used.^{15–17} On the other hand, a controlled release system is undoubtedly necessary for the delivery of expensive and less stable agents, such as growth factors. The application of biodegradable porous membranes loaded with CTGF to deliver them in a tightly regulated manner could be a good approach for promoting diabetic wound healing. In order to ensure the successful encapsulation and controlled delivery of the active agent inside the wound coverage matrix, a rational design of the polymeric carrier is required. Polymeric hydrogels such as poly(vinyl alcohol) (PVA) can effectively encapsulate and deliver active agents including growth factors.¹⁸ Due to its biodegradability, biocompatibility, low cost and ease of processing, PVA has received wide acceptance for various biomedical applications,¹⁹ particularly in wound dressing applications.^{20,21} However, the ability of PVA to hold the growth factor in the matrix and release it in a controlled manner is limited due to the quick swelling of its amorphous matrix. A thin coating of a relatively hydrophobic polymer over a PVA hydrogel could be a novel approach to protect the loaded growth factor and facilitate its controlled release. Poly(lactic acid) (PLA) can be a good candidate for the coating because of its biodegradability, biocompatibility and hydrophobicity.^{22,23} PLA is already being used in biomedical applications such as tissue engineering scaffolds, wound dressings, drug delivery systems and sutures.^{24–26}

Electrospinning is the most promising technique used to produce highly porous fibrous membranes for various biomedical applications.^{27–29} This process has been successfully exploited for the generation of continuous, ultra fine fibers from polymers like poly(vinylidene fluoride-trifluoroethylene) (P(VDF-TrFE)),^{30,31} polycaprolactone (PCL),^{32,33} polyvinyl alcohol (PVA),³⁴ gelatin³⁵ and have been used for a diverse range of medical uses.^{36,37} Coaxial electrospinning is a relatively recent approach to fabricate fibers from two different polymers where one polymer forms the core and the other forms the shell or sheath.^{38–40} In order to obtain PVA fibers (loaded with CTGF) coated with PLA, coaxial electrospinning was used in this study.

In this work, we report the development of electrospun membranes composed of core-shell fibers loaded with CTGF for diabetic wound healing applications. The major rationale of this work was to design core-shell structured fibers in such a way that the loaded CTGF in the PVA core component would be released in a sustained manner for an extended time period through the pores of the PLA shell. Using a core-shell structure composed of a PVA core containing CTGF and a PLA shell that regulate release is an effective way for the sustained delivery of CTGF, providing a long-term effect and to prevent overdoses. To our knowledge, fabrication of PVA-PLA core-shell fibers loaded with CTGF and their application in diabetic wound healing have not been reported yet. Herein, we hypothesize that the controlled release of CTGF from core-shell fibers could promote fibroblast, keratinocyte and endothelial cell proliferation/migration and angiogenesis which could result in the rapid healing of diabetic wounds. Developed membranes were tested for morphological, physicochemical and biological properties. Results of this study demonstrated that the presence of CTGF in the membranes can enhance cell proliferation, cell migration and angiogenesis which may improve diabetic wound healing.

Materials And Methods

Materials

Polyvinyl alcohol (PVA, M_n 90×10^3 – $80 \times 10^3 Da$), CTGF, dichloromethane and 3-(4,5-dimethylthiazol-2-yl)-2,5-diphenyltetrazolium bromide (MTT) used in this work were purchased from Sigma-Aldrich. Poly-L-lactic acid (PLLA, M_n 125×10^3 – $120 \times 10^3 Da$) was obtained from Akina, US. Phosphate buffered saline (PBS), keratinocyte serum free medium, penicillin-streptomycin solution and

bovine pituitary extract (BPE) were obtained from Gibco. Live/Dead assay kits, DAPI (4',6-diamidino-2-phenylindole) and phalloidin stains were obtained from Invitrogen.

Fabrication Of PLA-PVA-CTGF Electrospun Membranes

For the preparation of the membranes, a specific quantity of CTGF was accurately weighed to obtain an effective CTGF content in a PVA matrix and was ultra-sonicated for 15 mins to thoroughly disperse them in PBS. Details of the optimization of the coaxial electrospinning process were given in an earlier publication.⁴¹ The required amount of PVA pellets were dissolved in hot deionized water. Then, the prepared PVA solutions were mixed with a CTGF solution to get a 6% w/v PVA solution containing 0.1% w/w of CTGF. For the PLA shell, a 10% PLLA solution was made in a DCM/DMF (1:9 ratio) mixed solvent system. The electrospinning set up comprised of two syringe pumps (infusion) with 10 mL syringes containing polymer solutions, a high voltage power supply providing a 15 kV DC voltage and a stationary collector. Syringes were connected to a coaxial needle in such a way that the PVA or PVA-CTGF solution came out through the inner tube and PLA came out thorough the outer tube of the coaxial needle. The flow rate of PVA and PLA solutions was 0.5 mL h⁻¹ and 3 mL h⁻¹, respectively. The tip to collector distance was maintained as 10 cm throughout the experiment.

Characterization Of The PLA-PVA-CTGF Electrospun Membranes

SEM Analysis

The morphology of the developed membranes was examined using a scanning electron microscope (SEM). Gold coated core-shell membranes were imaged using FEI, Nova NanoSEM, 450 FE-SEM at 10 kV. The fiber diameter was calculated from the SEM images by using ImageJ software.

Thermal Analysis

The thermal analysis was conducted by using Differential Scanning Calorimetry (DSC) on pure PLA, PVA and PLA-PVA core-shell structures and PLA-PVA-CTGF core-shell structures under nitrogen flow. The nanofiber mats were weighed in the range between 6–8 mg and then placed in the aluminum pans. Then, it was loaded in a Perkin Elmer Pyris 7 DSC and provided with increasing temperature from 24 °C to 300 °C at a heating rate of 10 °C/min. After a 1 min hold at 300 °C, pans containing samples

were cooled to 24 °C. After a hold of 1 min, samples were again heated to 300 °C.

Fourier-Transform Infrared Spectroscopy (FTIR)

FTIR analysis was used to determine the specific chemical composition of pure PLA, PVA and PLA-PVA core-shell structures and PLA-PVA-CTGF core-shell structures. The FTIR measurements were conducted using a PerkinElmer (USA), Spectrum 400 FTIR instrument.

Mechanical Properties Of The PLA-PVA-CTGF Membranes

To determine the tensile properties of PLA-PVA and PLA-PVA-CTGF membranes, uniaxial tensile tests were performed using a Tinius Olsen H50 KT Universal Testing Machine (UTM) as per the standard procedure (ASTM D 882). Rectangular shaped membranes with 6×1 cm² dimensions were used for the measurements. The experiments were conducted by keeping a 3 cm gauge length. The machine operated at a speed of 1 mm/min and applying a 500 N mechanical loading on the samples.

Swelling Studies

In order to avoid excess exudates produced by the wounds, wound healing patches should have an optimal exudate uptake capacity. For that reason, swelling studies were performed on PLA-PVA and PLA-PVA-CTGF membranes. The membranes were cut into a size of 2 cm in length and 2–3 cm in width. The weight was measured before and after immersing in PBS at different time frames (0.5 to 144 h). The following Equation (1) was used to determine the water uptake capacity of the samples:

$$\text{Percentage of Swelling} = \frac{[(\text{Wet weight} - \text{Dry weight})/\text{Dry weight}] \times 100}{1} \quad (1)$$

In Vitro CTGF Release

In vitro release studies were performed according to an earlier report with slight modifications.⁴² Briefly, electrospun membranes weighing about 50 mg were placed in 12-well plates filled with 3 mL DMEM medium and kept in an incubator set to 37°C temperature. At predetermined time points, 400 µl of the release medium was retrieved from each well and replaced by 0.4 µl of fresh release medium. The collected release medium was used for protein determination. The concentration of growth factors in the supernatant was determined using a Pierce BCA protein estimation kit (Thermo Scientific) microplate method.

In Vitro Cell Culture Studies

Viability Staining For Cytotoxicity Analysis

3T3 fibroblasts (ATCC CRL-1658, Passage-48), HaCat keratinocytes (Passage-54) and EA.hy926 endothelial cells (ATCC CRL-2922, Passage-27) were seeded on pre-sterilized and pre-wetted scaffolds. The membranes were cut into a 1 x 1 cm size and cells were seeded at a final concentration of 2×10^4 cells/sample and cultured in 24-well plates. Both 3T3 fibroblasts and HaCat keratinocytes were maintained in DMEM (Gibco, Ireland) provided with 10% fetal bovine serum and a penicillin/streptomycin solution (Gibco, US origin). EA.hy926 endothelial cells were maintained in endothelial cell medium (Gibco, Ireland). All the cell seeded membranes were incubated in an incubator with a 5% CO₂ supply for 24 h, 3 days and 7 days. The LIVE/DEAD Cell Imaging Kit (488/570) was used for the assay according to the protocol described by the manufacturer (Molecular Probes, Invitrogen, USA). After the incubation period, the cells were washed with DPBS and then the prepared reagent (100 µl) was added to each well. After 30 min of incubation at 38°C, the fluorescence images were taken using an Olympus, FV300 microscope.

Cell Viability Assay

The effect of PLA-PVA and PLA-PVA-CTGF membranes on mouse NIH 3T3 fibroblast, human HaCat keratinocyte and human EA.hy926 endothelial cell proliferation were assessed using MTT cell viability assays. The membranes were cut into a 1 x 1 cm size and cells were seeded at a final concentration of 2×10^4 cells/sample and cultured in 24-well plates. The cell density was 2×10^4 cells/well in a 24 well plate and cultured under appropriate conditions as described in the previous section. All the cell seeded membranes were incubated in an incubator with a 5% CO₂ supply for 24 h, 3 days and 7 days, and MTT assays were performed according to the manufacturer's protocol (Molecular Probes, Invitrogen, USA). Absorbance was recorded at 570 nm using an Infinite F200 PRO (Tecan, Switzerland) microplate reader. All experiments were repeated for a minimum of three times.

To calculate the effect of the scaffolds on cell viability, Equation (2) was used:

$$\text{Cell proliferation(\%)} = \frac{(\text{OD of sample}/\text{OD of control})}{X 100} \quad (2)$$

In Vitro Wound Healing Assay

An in vitro wound healing assay was performed by a wound-healing scratch assay as described in.⁴³ In brief, 3T3, HaCat

or EA.hy926 cells were seeded in a 12 well plate at a density of 5×10^4 cells/well. When the cells reached confluency, a scratch was made with the help of a 100 µL pipette tip. In each well, pre-sterilized scaffolds (1x1 cm) were added. The images were taken initially at the time of placing the membranes and after 24 h with an Olympus inverted fluorescent microscope (Olympus, UK). The wound contraction was measured from the images using ImageJ software and the scratch contraction (%) was determined using Equation (3):

$$\text{Scratch contraction (\%)} = (Wd^0 - Wd^t) / Wd^0 \times 100 \quad (3)$$

Where Wd^0 and Wd^t are the gap between scratch edges before and after time "t" of incubation with the samples, respectively.

Angiogenic Properties Of The Developed Core-Shell Membranes Using The CAM Assay

For the CAM assay, fertilized chicken (*Gallus domesticus*) eggs were purchased from Arab Qatari Poultry Production Co. The eggs were incubated until day 4 at 37 °C from the day of fertilization in a humidified egg incubator (The Sportsman, Brookfield). After the incubation, the eggs were taken out and cleaned with 70% ethanol. A circular window was made from the broad edge of the egg with the help of a scissor. A 1 cm² PLA-PVA and PLA-PVA-CTGF electrospun membrane was placed on the exposed surface of CAM. The exposed window was covered with transparent adhesive tape. Then, it was again placed in a humidified 40% incubator at 37 °C. After 24 h, the vascular development on the CAM was observed with a stereo microscope and the number of branching points and diameter of vessels were quantified using Angioquant software.

Statistical Analysis

Unless specified, all the experimental procedures were carried out in triplicate and the results were reported in terms of means and standard deviation. Statistical significance between different groups were analyzed by a Student's *t*-test using Minitab statistical software from the means of each group (* P < 0.05 was considered as statistically significant).

Results

Characterization Of PLA-PVA-CTGF Scaffolds

SEM analysis was performed to determine the morphological features of PLA-PVA and PLA-PVA-CTGF membranes. The

obtained PLA-PVA and PLA-PVA-CTGF membranes were highly porous and composed of randomly oriented fibers with apparently the same individual fiber diameters (Figure 1A and B). Neither of the membranes showed beads or irregularities in/on the fibers. However, the surface of the individual fibers was highly porous in nature. The average fiber diameters were calculated from the SEM micrographs (data not shown). The average individual fiber diameter of neat PLA-PVA membranes was $2.6 \pm 1.4 \mu\text{m}$. We did not observe a considerable difference between the fiber morphology and diameters of the PLA-PVA and PLA-PVA-CTGF membranes.

The XRD patterns of the PLA, PVA, PLA-PVA and PLA-PVA-CTGF membranes are shown in Figure 1C. The PLA samples exhibited an intense diffraction peak at 2θ of 16.8° indicating the presence of (110/200) planes and the other less prominent peak observed at 19.1° corresponding to the (010) plane.⁴⁴ In addition, a minor peak at 14.5° corresponding to the (010) plane was also observed.⁴⁵ The XRD profile of the PVA showed an intense peak with a maxima at 2θ 19.7° and a shoulder peak at 2θ 22° were present.⁴⁶ The PLA-PVA core-shell membranes showed prominent peaks of PLA. Apart from the diffraction patterns of PLA, one major peak of PVA which was centered around 19.7° was also observed in the core-shell membranes (marked by arrows in Figure 1C). We did not observe a remarkable difference in the XRD patterns of PLA-PVA and PLA-PVA-CTGF membranes.

FTIR analysis in attenuated total reflectance (ATR) mode was used to examine the surface chemistry of PLA, PVA, PLA-PVA and PLA-PVA-CTGF fibers (Figure 1D). PVA fibers showed the characteristic peaks of hydroxyl groups at $3200\text{--}3600 \text{ cm}^{-1}$, however, which were mostly not observed in the core-shell fibers. The presence of hydroxyl peaks observed in certain samples of the PLA-PVA and PLA-PVA-CTGF core-shell fibers might be due to the presence of PVA or the PVA-CTGF core component exposed to the outside of the PLA fibers through the pores present on the surface. This indicated that PVA was not exposed on the surface of the core-shell fibers due to the presence of a PLA shell on the surface of the fibers. This indicated the successful formation of the core-shell fibers.

Figure 1E and F show the DSC heating and cooling thermograms of the developed membranes. The melting peak of PVA, which is about 220°C according to the DSC curve, was shifted to a low temperature in the heating curves of the PLA-PVA core-shell fibers due to the

restriction of PVA chain mobility by PLA chains. Further, the increased interaction that might exist between the polymer chains of PLA and PVA impedes the crystallization of both PLA and PVA, which can also be apparent from the less intense crystallization peaks in the cooling curves. Meanwhile, the crystallization of PVA in the core-shell fibers was further retarded due to the presence of CTGF. However, there was no significant effect on the melting transition of the PLA-PVA core-shell fibers due to the CTGF loading.

Tensile Properties Of The Membranes

Figure 2A–D shows the representative tensile stress–strain curves and corresponding tensile properties of the developed membranes. From the stress–strain curves, it was apparent that PLA exhibits a typical stress–strain behavior with a linearly elastic region at low strain, followed by the plastic deformation before breaking. Fracture strain and yield stress of pure PLA were 80% and 2.8 MPa, respectively. PVA membranes demonstrated an elongation at break and ultimate tensile stress of $38.5 \pm 8.8\%$ and $1.9 \pm 0.6 \text{ MPa}$, respectively. However, PLA nanofibers showed a high tensile strength and tensile modulus when compared with PVA or PLA-PVA membranes, which could be attributed to the difference in molecular organization within the polymer itself. The tensile moduli values of PVA was 43.48 ± 7.31 , whereas the stress at break was $2.05 \pm 0.37 \text{ MPa}$. These results are in good agreement with earlier studies.⁴⁷

Both PLA-PVA and PLA-PVA-CTGF membranes showed 73.08 ± 9.12 and $70.14 \pm 11.23\%$ maximum elongation, respectively. Core-shell PLA-PVA and PLA-PVA-CTGF membranes showed an ultimate tensile stress of $2.62 \pm 1.22 \text{ MPa}$ and $3.12 \pm 2.18 \text{ MPa}$, respectively. Relatively similar tensile properties were observed for core-shell PLA-PVA membranes with and without CTGF indicating that the addition of a small quantity of CTGF did not affect the elastic properties of the membranes. Young's moduli were apparently the same for all the studied samples except bare PLA.

Exudate Uptake Capacity And CTGF Release

Swelling of PLA-PVA-CTGF membranes were examined to understand their exudate uptake capacity. Water uptake capacity of PLA, PVA, PLA-PVA and PLA-PVA-CTGF membranes are shown in Figure 3A. The neat PLA

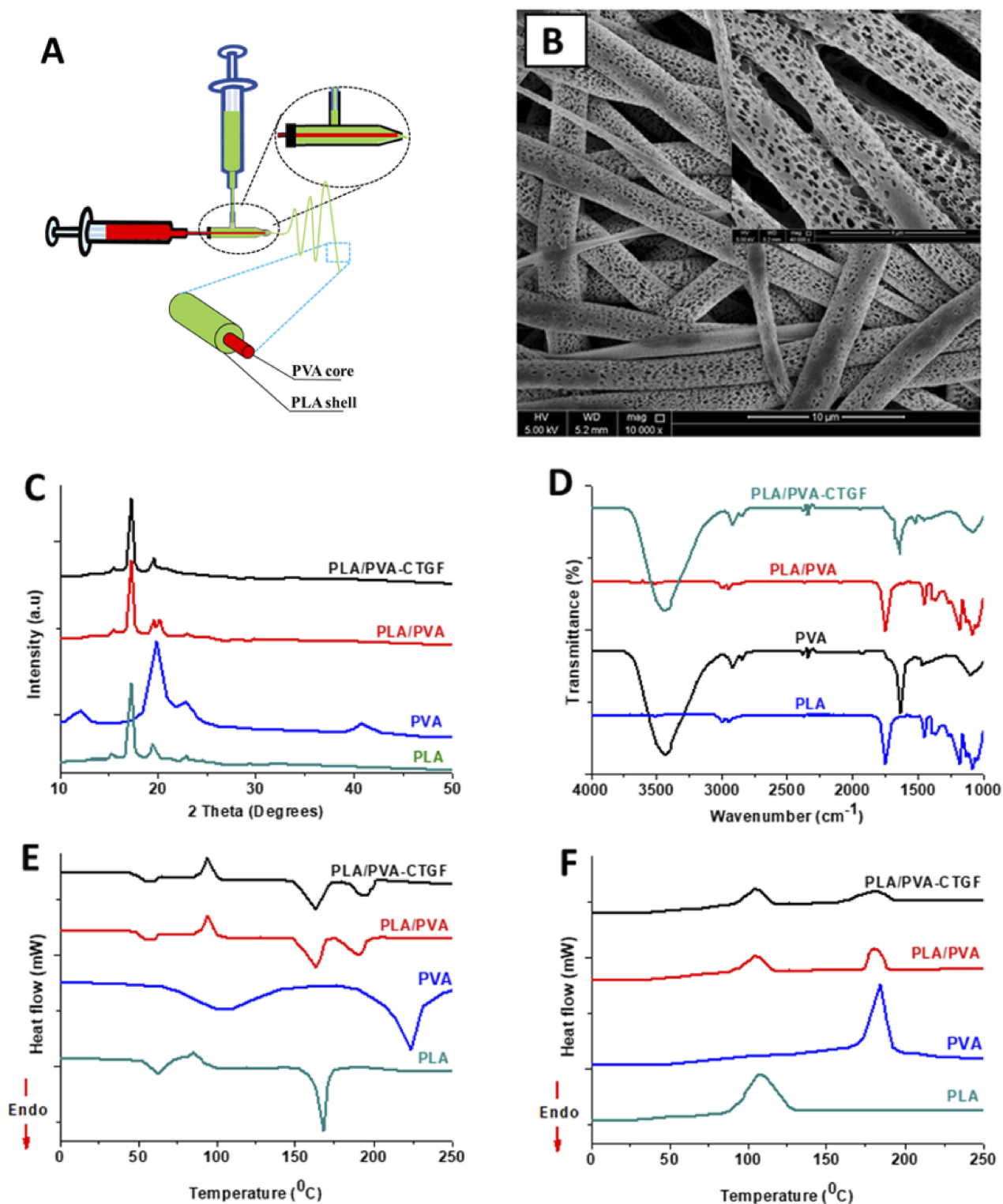


Figure 1 Results of morphological and physical characterization of the developed core-shell fiber-based membranes. Schematic representation of the fabrication process of the core-shell membranes (A). SEM image of coaxial PLA-PVA-CTGF membranes showing the morphology (B). XRD patterns (C), FTIR spectra (D), DSC heating thermogram (E) and DSC cooling thermogram (F) of fabricated membranes.

membrane showed low water uptake throughout the study period which was about 25–30%. Neat PVA membranes showed an initial sudden swelling. It reached up to the

peak of $275 \pm 38\%$ within 10 h of the study, then declined slowly. This might be due to the dissolution of PVA fibers in water. In the case of PLA-PVA-CTGF, a gradual

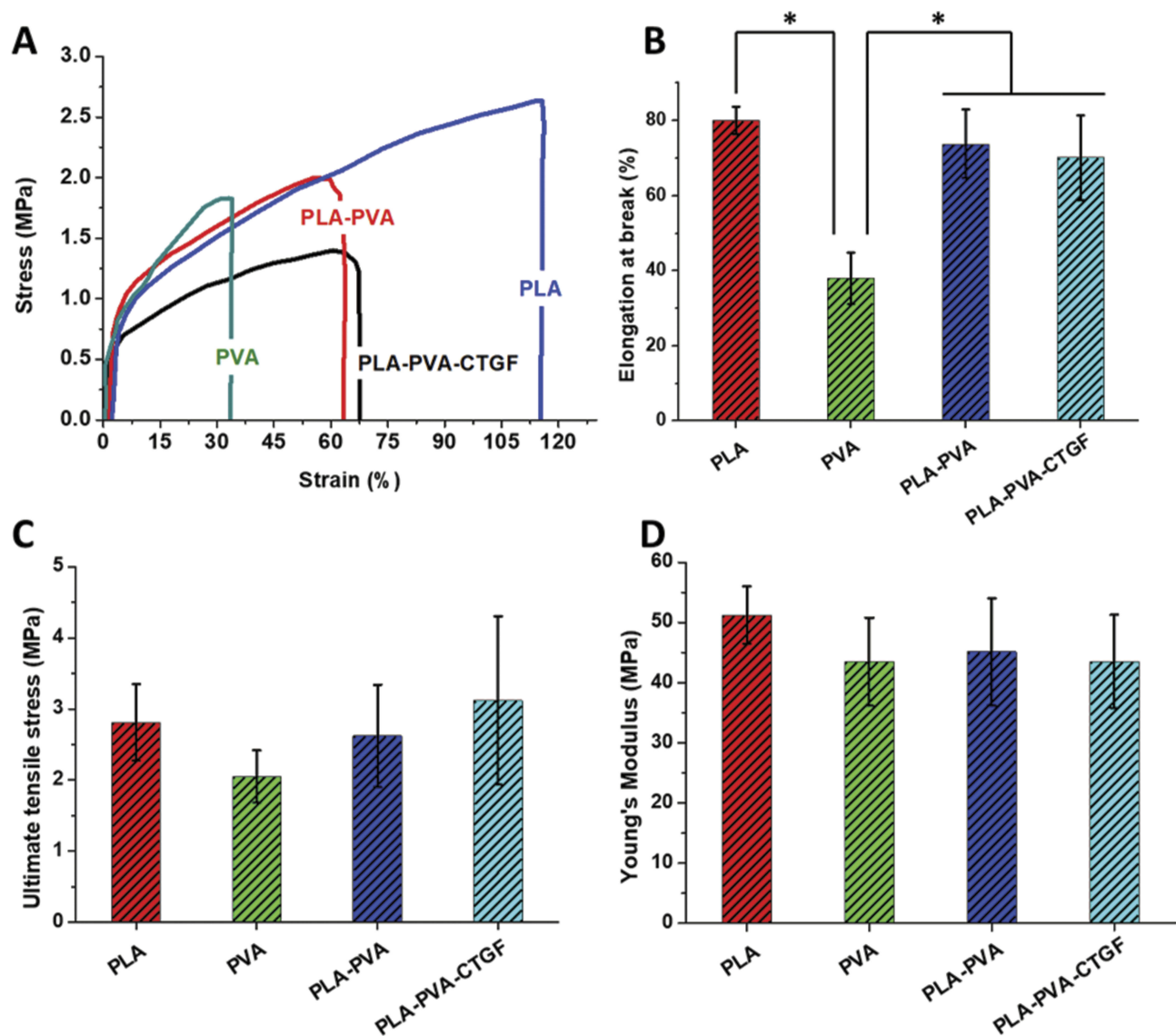


Figure 2 Mechanical testing results of the developed membranes. Stress-strain curve (A), Elongation at break (B), Ultimate tensile stress (C) and Young's modulus (D) of PLA, PVA, PLA-PVA and PLA-PVA-CTGF membranes. P-values were calculated using Student's t-test where (*) indicates a significant difference from other group of comparison ($p \leq 0.05$).

increase in the water uptake was observed within 0–1 h of the study which further improved gradually and reached a peak uptake ranging from 74 to 95% at about 72 h of the study. As evident for the obtained data, both PLA-PVA and PLA-PVA-CTGF core-shell fibers were able to absorb a good amount of water while being stable in water.

The combination of transient and prolonged release in the early stages and later stages of wound healing, respectively, is normally desirable for tissue regeneration. The release profile of CTGF from core-shell fibers is shown in Figure 3B. The concentration of CTGF, measured for 15 days, clearly indicates that the release was in a sustained manner. The initial release (for the first 24h) was

comparatively higher compared to longer time points. However, the release of CTGF was retained even after 15 days of the experiment.

CTGF Loaded Membranes Showed Higher Fibroblast, Keratinocyte And Endothelial Cell Viability Live-Dead Staining

For the successful application of the developed membranes as a wound dressing, native cells such as fibroblasts, keratinocytes and endothelial cells should present sufficient cell viability. The observed live and dead cells

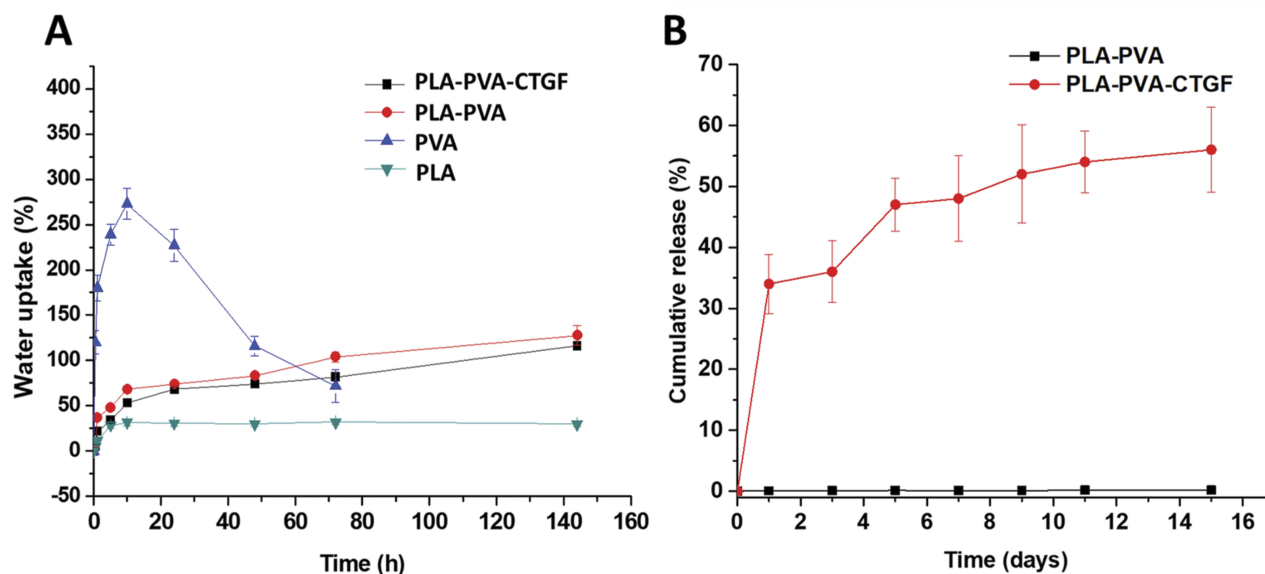


Figure 3 Water uptake capacity (A) and cumulative release (B) of PLA-PVA-CTGF membranes.

on the PLA-PVA and PLA-PVA-CTGF membranes are given in [Figure 4A](#). Fibroblast cells on the PLA-PVA membranes showed a slightly smaller number of live (green) cells as the green fluorescence was less in this case. In contrast, fibroblast cells cultured on the CTGF loaded membranes showed several green colored cells compared to the controls and membranes without CTGF. There was no considerable difference in dead fibroblast cells (red colored) between the different treatment groups. Almost all of the HaCat keratinocyte cells cultured with the membranes were viable irrespective of their composition. In contrast, EA.hy926 endothelial cells showed a considerable difference between the different sample treatment groups. A higher number of live cells were observed on those cells treated with PLA-PVA-CTGF membranes compared to the neat PLA-PVA membranes. However, we did not observe considerable variation in relative ratios of live and dead cells, which indicated the non-toxicity of all the tested membranes. The adhesion and proliferation of fibroblasts, keratinocytes and endothelial cells on the fibers are given in [Figure S1](#).

Cell Viability By MTT Assay

To determine cell viability and growth of mammalian cells on the developed membranes, 3T3 fibroblasts, HaCat keratinocytes and EA.hy926 endothelial cells were seeded on the membranes and MTT assays were performed. The obtained results are given in [Figure 4B](#). During the 7 days of the study period, PLA-PVA membranes were

cytocompatible, and possessed a comparable viability with the control. PLA-PVA-CTGF membranes showed greater cell viability compared to the bare PLA-PVA membranes and control especially in the case of 3T3 fibroblasts and HaCat keratinocytes. About a $113.5 \pm 4.5\%$ viability was observed on PLA-PVA-CTGF at 24h, which was significantly different from the PLA-PVA treated cells. On day-3 and day-7 after treatment, PLA-PVA-CTGF treated fibroblasts showed a $115.7 \pm 5.4\%$ and $117.4 \pm 2.3\%$ viability compared to the control, respectively. From this, it was clear that there was no considerable variation in cell viability with treatment time. However, EA.hy926 endothelial cells cultured on the different membranes did not show intergroup differences in viability up to 3 days of cell culture. However, on the 7th day of treatment, a significant difference in cell viability was observed for PLA-PVA and PLA-PVA-CTGF membranes compared to the earlier treatment periods. Moreover, the viability of endothelial cells cultured on PLA-PVA-CTGF membranes was higher on the 7th day of treatment compared to the PLA-PVA membranes and controls. Overall, these findings indicated that the developed membranes loaded with CTGF are cytocompatible and are able to support fibroblast, keratinocyte and endothelial cell growth *in vitro*.

In Vitro Wound Healing

The migration of 3T3 fibroblasts, HaCat keratinocytes and EA.hy926 endothelial cells in the presence of the CTGF

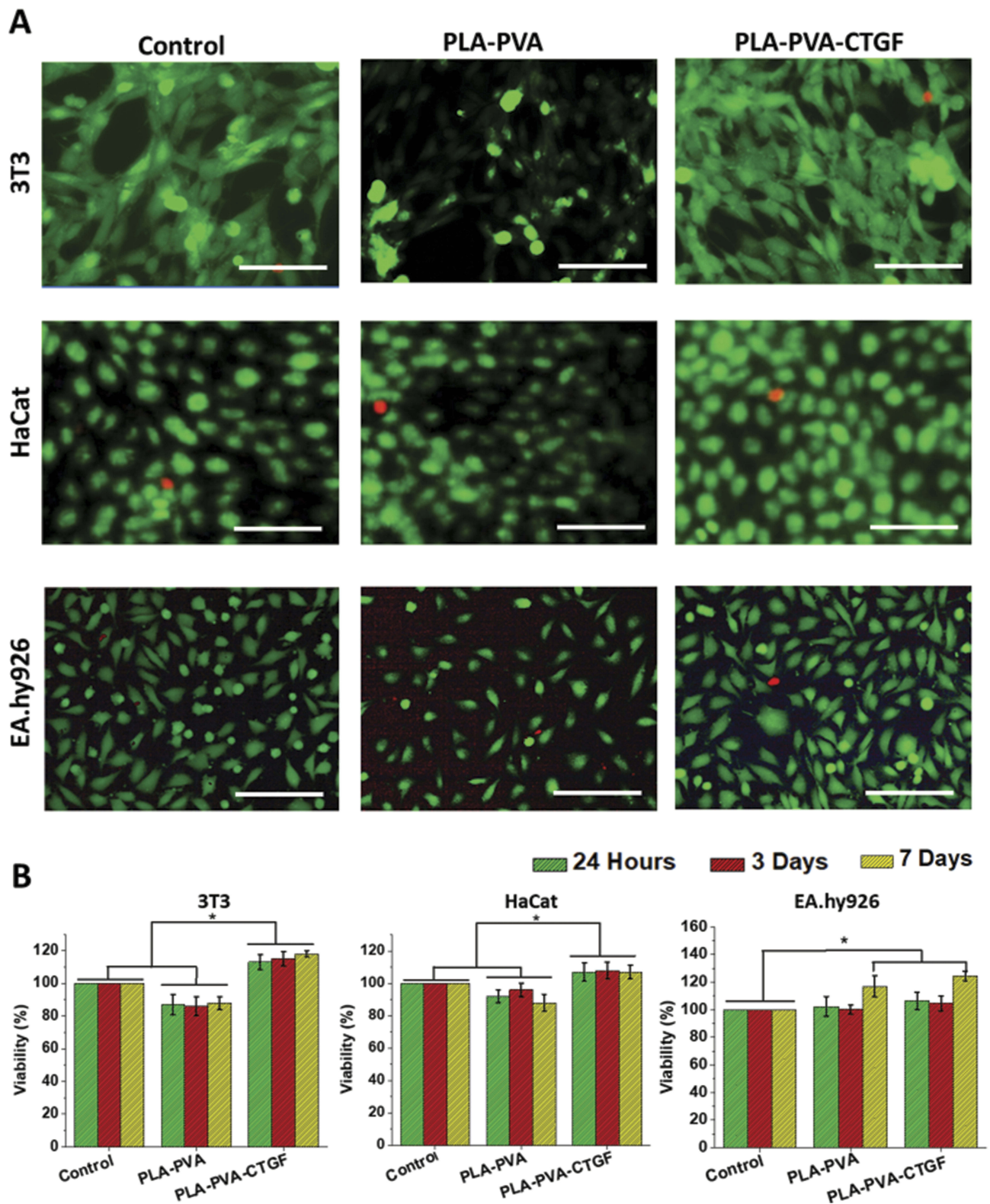


Figure 4 Results of in vitro cell culture studies on the developed membranes. Live/Dead assay results showing the viability of 3T3 fibroblasts, HaCat keratinocytes and EA.hy926 endothelial cells which were cultured with the PLA-PVA and PLA-PVA-CTGF membranes (A). Scale bars = 200 μm. Viability of 3T3, HaCat and EA.hy926 cells upon culturing with the scaffolds (B). P-values were calculated using Student's t-test where (*) indicates a significant difference from the other group of comparison ($p \leq 0.05$).

loaded membranes was assessed using an in vitro cell migration assay (Figure 5). Wounds generated on controls and

PLA-PVA membrane-treated 3T3 cells showed a wound contraction of $32.51 \pm 6.44\%$ and $36.08 \pm 4.67\%$,

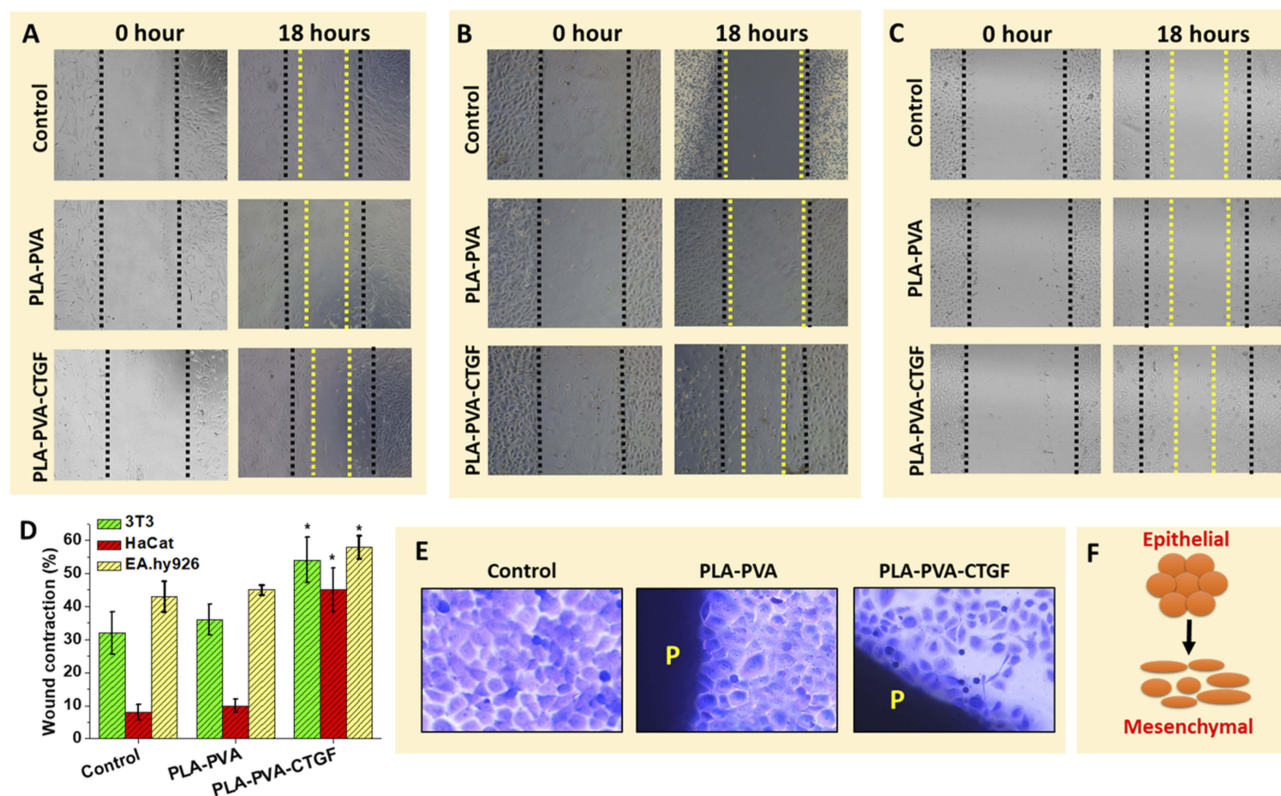


Figure 5 Results showing the effect of PLA-PVA and PLA-PVA-CTGF scaffolds on in vitro wound healing using 3T3 fibroblasts (A), HaCat keratinocytes (B) and EA.hy926 endothelial cells (C). Wound contraction (%) after treatment with the developed membranes (D). Morphological changes in HaCat cells which were incubated with PLA-PVA and PLA-PVA-CTGF membranes (E). Schematic representation of phenotypic changes of keratinocyte cells upon incubation with PLA-PVA-CTGF scaffolds (F). P-values were calculated using a Student's t-test where (*) indicates a significant difference from the control ($p \leq 0.05$). The images were taken at 100X magnification.

respectively (Figure 5A, D). There was no significant difference between the control and PLA-PVA groups. However, the PLA-PVA-CTGF membrane treated 3T3 cells showed a $54.34 \pm 6.8\%$ wound contraction. In the case of HaCat cells, the scratch closure was generally slow where a $8.62 \pm 2.34\%$ and $10.73 \pm 2.04\%$ contraction was only observed on the control and PLA-PVA treated cells (Figure 5B, 5D). However, the PLA-PVA-CTGF treated membrane groups showed a $45.54 \pm 6.68\%$ in vitro wound closure which was significantly different from controls and neat PLA-PVA treated cells. Therefore, the presence of bare membranes did not impair the normal in vitro migration rate of 3T3 and HaCat cells. We also examined the potential of the developed membranes to promote endothelial cell migration using an in vitro wound contraction assay. The contraction of a scratch with the PLA-PVA membrane was about $45.47 \pm 1.50\%$, while, the closure of the scratch with the control was $43.45 \pm 4.58\%$ (Figure 5C and D). There was no significant difference found in the healing of the scratch with the PLA-PVA membranes and the controls. However, the CTGF loaded PLA-PVA membranes showed a significant difference in wound

contraction which was about $58.64\% \pm 3.46\%$. Figure 5E and F show the variation in the morphology of keratinocytes upon incubation with PLA-PVA and PLA-PVA-CTGF membranes. Unlike the cells grown in the presence of PLA-PVA membranes, those grown in the presence of PLA-PVA-CTGF membranes had an elongated cell morphology.

PLA-PVA-CTGF Membranes Showed Higher Angiogenesis In A CAM Model

The effect of the developed membranes on angiogenesis was evaluated by an in ovo chicken chorioallantoic membrane (CAM) assay. Figure 6A shows the appearance of a network of blood vessels growing around the PLA and PLA-PVA membranes. As a control, PBS showed no effect on angiogenesis. It is evident from the results that the PLA-PVA-CTGF membranes have a higher ability to promote angiogenesis compared to the other samples. Similarly, CTGF loaded membranes exhibited more angiogenesis by showing an increased number of blood vessels around the PLA-PVA-CTGF membranes (Figure 6B). In addition, significantly higher blood vessel diameters were

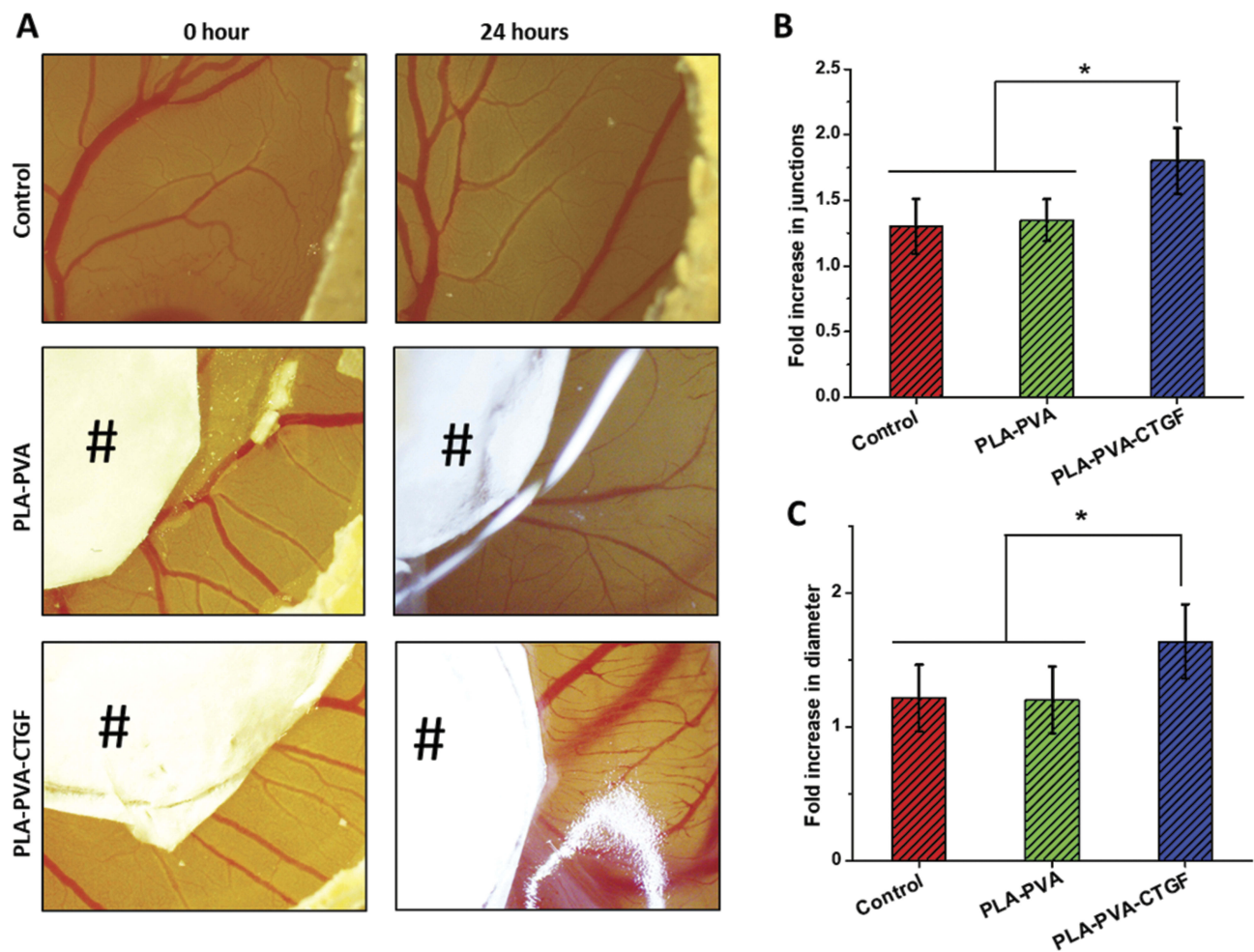


Figure 6 Effect of PLA-PVA-CTGF on angiogenesis in vivo was evaluated by in ovo model of chicken chorioallantoic membrane (CAM) assay (A). Fold increase in blood vessel junctions (B) and fold increase in blood vessel diameter (C) after 24 hrs of treatment with samples. # indicates the core-shell membranes. P-values were calculated using one-way ANOVA where (*) indicates a significant difference from the other group of comparison ($p \leq 0.05$). The images were taken at 10X magnification.

also observed for the PLA-PVA-CTGF membranes compared to the control (Figure 6C).

Discussion

Electrospun membranes have been widely investigated for wound dressing and tissue engineering applications with several promising outcomes.⁴⁸ Major advantages of electrospun membranes that make them suitable for wound coverage applications are good elasticity, a high surface area to volume ratio, high air permeability and the extracellular matrix mimicking morphology. Here in this research, we developed electrospun core-shell membranes based on PVA and PLA where the growth factor, CTGF, was loaded in the PVA core. We performed initial optimization studies to determine the optimum electrospinning parameters, such as applied voltage, flow rate, solvent polarity, solvent volatility, solution concentration, temperature and humidity. It was

observed from the SEM images that the obtained PLA-PVA membranes were composed of submicron fibers with a highly porous architecture (about 80% porosity based on the alcohol diffusion method) and individual fibers with almost similar diameters. Such a high porosity of the fibers facilitates appropriate oxygen and water permeability⁴⁹ while preventing the entry of microbes to the wounds.⁵⁰ Secondary pore formation was also observed on the individual fibers. We have observed that humidity played a critical role in the formation of secondary pores on fibers. At a relatively high humidity in the spinning environment, breath-moisture based pore formation can happen due to the condensation of droplets from the air and subsequent difference in the rate of evaporation of the solvent from the surface.⁵¹ It has already been reported that such secondary pore formation could be highly advantageous for providing appropriate nanotopographical^{52,53} and textural cues for cell adhesion

and proliferation on the fibers.⁵⁴ As a novel aspect of this study, pores present in the PLA shell facilitate the sustained release of CTGF. Electrospinning has been employed as a versatile technique to fabricate delivery vehicles for various drugs and biomolecules.⁵⁵ Biomolecules (such as growth factors) that are susceptible for denaturation in the presence of organic solvents which are used in conventional electrospinning can be loaded in fibers produced by coaxial electrospinning. During coaxial electrospinning, hydrophilic proteins can be preserved in the core water phase of fibers and their bioactivity could be retained to a large extent. The presence of a porous shell of PLA over the CTGF loaded PVA core could provide a sustained release of CTGF for an extended period. Information on the formation of the core-shell structure of PLA-PVA membranes was obtained from XRD analysis. Core-shell membranes have shown the presence of prominent peaks of PLA with less intense peaks for PVA. The absence of FTIR peaks corresponding to the hydroxyl groups of PVA in the core-shell fiber membranes indicate the successful formation of core-shell structures. The crystallization of PVA in the core-shell fibers was slightly affected in the PLA-PVA-CTGF membranes due to the presence of CTGF.

Sufficient elasticity and mechanical strength are required for a wound coverage matrix to prevent discomfort and failure during muscular movements. Bare PVA showed relatively less tensile strength since they were uncrosslinked.⁵⁶ The presence of a PLA shell over PVA improved the tensile strength of the PLA-PVA fibrous membranes. This might be due to the fact that more mechanically strong PLA coatings over PVA fibers prevented the failure of relatively weak PVA chains. The results of tensile testing revealed that the addition of CTGF had no significant influence on the tensile properties of PLA-PVA membranes. Owing to its adequate flexibility, elasticity and tensile strength, PLA-PVA-CTGF membranes can mechanically fit the defective areas and can avoid motion associated failure.

Effective wound management aims to produce a balance, ie a moist environment to promote healing but not so wet as to cause maceration and excoriation.⁵⁷ It is often difficult to select a dressing that is effective in healing, removes excess exudate and causes no trauma while also providing barrier functions until the wound is healed completely. In general, an optimum wound coverage material should provide a moist wound environment in the healing wound, offer protection from infections and support tissue regeneration.⁵⁸ They also should be able to absorb excess

wound exudates produced by the chronic wounds.⁵⁹ Thus, we evaluated the ability of PLA-PVA-CTGF membranes to absorb water to estimate its exudate management capacity. The neat PLA membrane showed low water uptake due to hydrophobic methyl groups in its structure. The limited water uptake shown by bare PLA could be initiated in the amorphous regions of PLA, since it is less organized and more accessible to water molecules.⁶⁰ Corroborating evidence from other studies on PVA-clay nanocomposites for wound dressing applications showed a relatively similar trend as observed in the current research.⁶¹ PLA-PVA-CTGF membranes had an appropriate capacity to hold large amounts of exudate which make them suitable candidates for even highly exudative wounds.

Furthermore, the gradual swelling behavior of PLA-PVA-CTGF membranes will be beneficial in continuously exuding wounds over a long duration.⁶² In addition, developed membranes will create a moist environment in the wound bed and support moist wound healing.⁶³ Moreover, surfaces with moderate hydrophilicity support the adsorption of proteins released from the cells and facilitate cell adhesion, while hydrophobic surfaces show poor cell attachment.⁶⁴ Since they are highly porous, they will be permeable to water and provide aeration.⁶⁵ However, the application of a PVA dressing with excess water content alone in the wound can lead to wound maceration.⁶⁶ Thus, PLA-PVA-CTGF dressings improve wound healing by providing a moist environment and absorbs excess wound exudate to prevent leakage. In order to obtain desirable bioactivity, loaded CTGF should be released in a controlled manner for prolonged time periods. The swelling PVA core might have resulted in the slow release of CTGF through the nanopores of a PLA shell in a sustained fashion. The initial burst release of CTGF from the PVA core could be associated with the fast dissolution of PVA from the pores which are directly exposed to the release medium. Such an initial higher release of protein from core-shell fibers was reported in earlier studies also.⁴¹ A subsequent slow release of CTGF from the PVA core can play a significant role in effective cell proliferation, angiogenesis and wound healing throughout the course of healing.

The viability and proliferation of cells such as fibroblasts, keratinocytes and endothelial cells within wound coverage matrices are important and have been established by several earlier studies.⁶⁷ CTGF plays several

key roles that will activate and protect fibroblasts from cell death.⁶⁸ Earlier reports suggest that the application of CTGF induces the expression of several genes including those coding MMP and support fibroblast survival and wound contraction.⁶⁹ The observed higher viability of fibroblast cells cultured with PLA-PVA-CTGF membranes could be ascribed to this protective effect of CTGF. Similarly, CTGF containing PLA-PVA membranes enhanced the viability of HaCat cells. However, the variation in the viability of endothelial cells was minimal between different membranes; such a cell specific differential effect of CTGF has been reported in earlier studies.^{70,71} For instance, CTGF protected chicken embryo fibroblasts from apoptosis⁷² whereas it induced apoptosis in human breast cancer cells.⁷³ This cell specific difference in the activity of CTGF might be the reason for the observed difference in cell viability observed here. Interestingly, PLA-PVA-CTGF core-shell membranes showed a higher viability in the studied cells even at the 7th day of treatment. The prolonged effect of enhanced cell proliferation on the CTGF loaded core-shell membranes could be due to the slow and sustained release of CTGF through the pores of the fibers. We also investigated the effect CTGF loaded membranes on the migration of important cells associated with wound healing such as fibroblasts, keratinocytes and endothelial cells. The migration of all the three types of cells and the contraction of the in vitro wounds were higher when CTGF loaded core-shell scaffolds were used. CTGF has been reported for its ability to promote the growth and migration of several types of mammalian cells such as vascular smooth muscle cells (VSMC),⁷⁰ human mesangial cells⁷¹ and endothelial cells.⁹ Fibroblasts and endothelial cells showed a marginal improvement in migration upon treatment with CTGF loaded membranes. However, keratinocytes showed a very pronounced effect in cell migration and wound contraction due to the treatment of CTGF loaded core-shell membranes. This considerable difference in the in vitro wound contraction behavior of keratinocytes might be due to the higher cell to cell adhesion and their less potency of migration.⁷² In order to promote cell migration in keratinocytes, tight cell-cell adhesion of keratinocytes should be disrupted with appropriate cues;⁷³ such signals (mostly growth factors and chemokines) can induce epithelial-mesenchymal transition (EMT) of keratinocytes which facilitate their migration and proliferation. Changes in the morphology of keratinocytes

treated with PLA-PVA-CTGF membranes indicated an EMT. Since re-epithelialization of wounds including chronic diabetic wounds depends upon the migration of keratinocytes from the cut margins of the wound, developed membranes containing CTGF with excellent cell migratory potential can be a good candidate for diabetic wound healing applications.

Inadequate angiogenesis plays an important role in the formation of non-healing diabetic wounds.⁷⁴ Due to the importance of promoting angiogenesis in diabetic wounds, we studied the angiogenic properties of the developed core-shell membranes. A superior angiogenic response was observed on chicken chorioallantoic membranes treated with PLA-PVA-CTGF membranes. Our results are in line with earlier reports regarding the angiogenic potential of CTGF.^{75,76} Higher endothelial cell migration, proliferation and survival are required for mitigating the impaired angiogenesis in diabetic wounds. PLA-PVA-CTGF induced modulation in endothelial cell viability and migration might have played a significant role in angiogenesis in chicken chorioallantoic membrane. We observed higher proliferation and migration of endothelial cells when cultured with CTGF containing PLA-PVA membranes. Earlier studies support our findings regarding the observed higher cell proliferation.⁷⁶ The present study further confirms the bioactivity of CTGF released from PVA core as evident from the increased blood vessel number and diameter based on the CAM model.

Overall, the obtained results demonstrate that the CTGF loaded core-shell fibers can have a significant positive impact on the viability and migration of multiple cells that are relevant in diabetic wound healing and facilitate subsequent wound contraction. Since the effective dose and duration of growth factor gradients are important factors that facilitate angiogenesis and wound healing, a slow release of CTGF might have significantly contributed to the overall performance of the developed membranes.⁷ Future studies should focus on the effect of PLA-PVA-CTGF on cell proliferation, angiogenesis, and wound closure rate in vivo using small animal models. Detailed investigations are also required to establish important parameters such as in vivo PLA-PVA degradation, in vivo CTGF release kinetics, and pharmacokinetics to further exploit the clinical potential of this bioactive wound dressing.

Conclusions

In this work, electrospun PLA-PVA core-shell membranes loaded with CTGF were developed and thoroughly characterized for morphological, physio-mechanical and biological

performance. SEM analysis provided the morphological characteristics of the developed membranes. FTIR and XRD analyses confirmed the formation of PLA-PVA core-shell fibers. Core-shell membranes possessed adequate elasticity, tensile strength, and tensile modulus to perform as an appropriate wound dressing. Fibroblasts, keratinocytes and endothelial cells were able to grow well on the CTGF loaded membranes. Results of the in vitro scratch assay shows that the membranes containing CTGF promoted cell migration and supported fast in vitro wound closure. CTGF loaded core-shell membranes have shown higher angiogenesis compared to the neat PLA-PVA membranes and controls. Overall, results indicated that CTGF loaded PLA-PVA core-shell membranes can be used for diabetic wound healing applications. However, detailed in vivo biocompatibility, hemocompatibility and wound healing studies need to be undertaken before considering the clinical application of the developed membranes.

Acknowledgments

This article was made possible by the NPRP9-144-3-021 grant funded by the Qatar National Research Fund (a part of the Qatar Foundation). We also acknowledge the support provided by the Central Laboratories Unit (CLU), Qatar University, Qatar. The statements made herein are solely the responsibility of the authors. The publication of this article was funded by the Qatar National Library. The authors also acknowledge Huseyin Cagatay Yalcin and Ala-Eddin Al Moustafa for sharing resources during the initial stage of this project.

Disclosure

The authors declare no competing interests in this work.

References

- Borys S, Hohendorff J, Frankfurter C, Kiec-Wilk B, Malecki MT. Negative pressure wound therapy use in diabetic foot syndrome— from mechanisms of action to clinical practice. *Eur J Clin Invest*. 2019;e13067. doi:10.1111/eci.13067
- Cunha M, Queirós P, Cardoso D, Santos E, Rodrigues M, Apóstolo J. The effectiveness of cleansing solutions for wound treatment: a systematic review. *JBIM Database System Rev Implement Rep*. 2014;12(10):121–151. doi:10.11124/jbisrir-2014-1746
- Xu F, Zhang C, Graves DT. Abnormal cell responses and role of TNF- α in impaired diabetic wound healing. *Biomed Res Int*. 2013;2013:1–9. doi:10.1155/2013/754802
- Bao P, Kodra A, Tomic-Canic M, Golinko MS, Ehrlich HP, Brem H. The role of vascular endothelial growth factor in wound healing. *J Surg Res*. 2009;153(2):347–358. doi:10.1016/j.jss.2008.04.023
- Hardwicke J, Schmaljohann D, Boyce D, Thomas D. Epidermal growth factor therapy and wound healing - past, present and future perspectives. *Surgeon*. 2008;6(3):172–177. doi:10.1016/S1479-666X(08)80114-X
- Pierce GF, Mustoe TA, Altrock BW, Deuel TF, Thomason A. Role of platelet-derived growth factor in wound healing. *J Cell Biochem*. 1991;45(4):319–326. doi:10.1002/jcb.240450403
- Li H, Cao C, Huang A, Man Y. Topically applied connective tissue growth factor/CCN2 Improves diabetic preclinical cutaneous wound healing: potential role for CTGF in human diabetic foot ulcer healing. *J Diabetes Res*. 2015;2015:1–3. doi:10.1155/2015/512959
- Kolluru GK, SC B, Kevil CG. Endothelial dysfunction and diabetes: effects on angiogenesis, vascular remodeling, and wound healing. *Int J Vasc Med*. 2012;2012:1–30. doi:10.1155/2012/918267
- Brigstock DR. Regulation of angiogenesis and endothelial cell function by connective tissue growth factor (CTGF) and cysteine-rich 61 (CYR61). *Angiogenesis*. 2002;5(3):153–165. doi:10.1023/A:1023823803510
- Hishikawa K, Nakaki T, Fujii T. Connective tissue growth factor induces apoptosis via caspase 3 in cultured human aortic smooth muscle cells. *Eur J Pharmacol*. 2000;392(1–2):19–22. doi:10.1016/S0014-2999(00)00115-1
- Shi-Wen X, Leask A, Abraham D. Regulation and function of connective tissue growth factor/CCN2 in tissue repair, scarring and fibrosis. *Cytokine Growth Factor Rev*. 2008;19(2):133–144. doi:10.1016/j.cytogfr.2008.01.002
- Frazier K, Williams S, Kothapalli D, Klapper H, Grotendorst GR. Stimulation of fibroblast cell growth, matrix production, and granulation tissue formation by connective tissue growth factor. *J Invest Dermatol*. 1996;107(3):404–411. doi:10.1111/1523-1747.ep12363389
- Nakerakanti SS, Kapanadze B, Trojanowska M, Ghatnekar A, Markiewicz M. Connective Tissue Growth Factor (CTGF/CCN2) mediates angiogenic effect of SIP in human dermal microvascular endothelial cells. *Microcirculation*. 2010;18(1):1–11. doi:10.1111/j.1549-8719.2010.00058.x
- Berlanga-Acosta J, Fernández-Montequín J, Valdés-Pérez C, et al. Diabetic foot ulcers and epidermal growth factor: revisiting the local delivery route for a successful outcome. *Biomed Res Int*. 2017;2017:1–10. doi:10.1155/2017/2923759
- Masood N, Ahmed R, Tariq M, et al. Silver nanoparticle impregnated chitosan-PEG hydrogel enhances wound healing in diabetes induced rabbits. *Int J Pharm*. 2019;559:23–36. doi:10.1016/j.ijpharm.2019.01.019
- Ahmed R, Tariq M, Ali I, et al. Novel electrospun chitosan/polyvinyl alcohol/zinc oxide nanofibrous mats with antibacterial and antioxidant properties for diabetic wound healing. *Int J Biol Macromol*. 2018;120:385–393. doi:10.1016/j.ijbiomac.2018.08.057
- Liu M, Zhang H, Min D, et al. Dual layered wound dressing with simultaneous temperature & antibacterial regulation properties. *Mater Sci Eng C*. 2019;94:1077–1082. doi:10.1016/j.msec.2018.09.049
- Zahid AA, Ahmed R, ur Rehman SR, et al. Nitric oxide releasing chitosan-poly (vinyl alcohol) hydrogel promotes angiogenesis in chick embryo model. *Int J Biol Macromol*. 2019;136:901–910. doi:10.1016/j.ijbiomac.2019.06.136
- Wang J, Cheng Q, Lin L, Jiang L. Synergistic toughening of bioinspired poly(vinyl alcohol)-clay- nanofibrillar cellulose artificial nacre. *ACS Nano*. 2014;8(3):2739–2745. doi:10.1021/nn406428n
- Kamoun EA, Kenawy ERS, Chen X. A review on polymeric hydrogel membranes for wound dressing applications: PVA-based hydrogel dressings. *J Adv Res*. 2017;8(3):217–233. doi:10.1016/j.jare.2017.01.005
- Hayes JC, Kennedy JE. An evaluation of the biocompatibility properties of a salt-modified polyvinyl alcohol hydrogel for a knee meniscus application. *Mater Sci Eng C*. 2016;59:894–900. doi:10.1016/j.msec.2015.10.052
- Hasan A, Soliman S, El Hajj F, Tseng YT, Yalcin HC, Marei HE. Fabrication and in vitro characterization of a tissue engineered PCL-PLLA heart valve. *Sci Rep*. 2018;8(1):8187. doi:10.1038/s41598-018-26452-y
- Gandolfi MG, Zamparini F, Degli Esposti M, et al. Poly(lactic acid)-based porous scaffolds doped with calcium silicate and dicalcium phosphate dihydrate designed for biomedical application. *Mater Sci Eng C*. 2018;82:163–181. doi:10.1016/j.msec.2017.08.040

24. da Silva D, Kaduri M, Poley M, et al. Biocompatibility, biodegradation and excretion of polylactic acid (PLA) in medical implants and theranostic systems. *Chem Eng J*. 2018;340:9–14. doi:10.1016/J.CEJ.2018.01.010
25. Han X, Wang D, Chen X, Lin H, Qu F. One-pot synthesis of macro-mesoporous bioactive glasses/polylactic acid for bone tissue engineering. *Mater Sci Eng C*. 2014;43:367–374. doi:10.1016/j.msec.2014.07.042
26. Childs A, Hemraz UD, Castro NJ, Fenniri H, Zhang LG. Novel biologically-inspired rosette nanotube PLLA scaffolds for improving human mesenchymal stem cell chondrogenic differentiation. *Biomed Mater*. 2013;8(6):065003. doi:10.1088/1748-6041/8/6/065003
27. Hasan A, Memic A, Annabi N, et al. Electrospun scaffolds for tissue engineering of vascular grafts. *Acta Biomater*. 2014;10(1):11–25. doi:10.1016/j.actbio.2013.08.022
28. Augustine R, Hasan A, Patan NK, et al. Cerium Oxide Nanoparticle Incorporated Electrospun Poly(3-hydroxybutyrate-co-3-hydroxyvalerate) Membranes for Diabetic Wound Healing Applications. *ACS Biomater Sci Eng*. 2019. doi:10.1021/acsbomaterials.8b01352
29. Tonsomboon K, Butcher AL, Oyen ML. Strong and tough nanofibrous hydrogel composites based on biomimetic principles. *Mater Sci Eng C*. 2017;72:220–227. doi:10.1016/j.msec.2016.11.025
30. Augustine R, Dan P, Sosnik A, et al. Electrospun poly(vinylidene fluoride-trifluoroethylene)/zinc oxide nanocomposite tissue engineering scaffolds with enhanced cell adhesion and blood vessel formation. *Nano Res*. 2017;10(10):3358–3376. doi:10.1007/s12274-017-1549-8
31. Augustine R, Sarry F, Kalarikkal N, Thomas S, Badie L, Rouxel D. Surface acoustic wave device with reduced insertion loss by electrospinning P(VDF-trFE)/ZnO nanocomposites. *Nanomicro Lett*. 2016;8(3):282–290. doi:10.1007/s40820-016-0088-2
32. Recek N, Resnik M, Motaln H, et al. Cell adhesion on polycaprolactone modified by plasma treatment. *Int J Polym Sci*. 2016;2016. doi:10.1155/2016/7354396
33. Augustine R, Kalarikkal N, Thomas S. Clogging-free electrospinning of polycaprolactone using acetic acid/acetone mixture. *Polym Plast Technol Eng*. 2016;55(5):518–529. doi:10.1080/03602559.2015.1036451
34. Alavarse AC, de Oliveira Silva FW, Colque JT, et al. Tetracycline hydrochloride-loaded electrospun nanofibers mats based on PVA and chitosan for wound dressing. *Mater Sci Eng C*. 2017;77:271–281. doi:10.1016/j.msec.2017.03.199
35. Butcher AL, Koh CT, Oyen ML. Systematic mechanical evaluation of electrospun gelatin meshes. *J Mech Behav Biomed Mater*. 2017;69:412–419. doi:10.1016/j.jmbbm.2017.02.007
36. Duque Sánchez L, Brack N, Postma A, Pigram PJ, Meagher L. Surface modification of electrospun fibres for biomedical applications: a focus on radical polymerization methods. *Biomaterials*. 2016;106:24–45. doi:10.1016/j.biomaterials.2016.08.011
37. Lee S-J, Nowicki M, Harris B, Zhang LG. Fabrication of a highly aligned neural scaffold via a table top stereolithography 3D printing and electrospinning. *Tissue Eng Part A*. 2016;23(11–12):491–502. doi:10.1089/ten.tea.2016.0353
38. Johnson R, Ding Y, Nagiah N, Monnet E, Tan W. Coaxially-structured fibres with tailored material properties for vascular graft implant. *Mater Sci Eng C*. 2019;97:1–11. doi:10.1016/j.msec.2018.11.036
39. da Silva TN, Gonçalves RP, Rocha CL, et al. Controlling burst effect with PLA/PVA coaxial electrospun scaffolds loaded with BMP-2 for bone guided regeneration. *Mater Sci Eng C*. 2019;97:602–612. doi:10.1016/j.msec.2018.12.020
40. Gonçalves RP, da Silva FFF, Picciani PHS, Dias ML. Morphology and thermal properties of core-shell PVA/PLA ultrafine fibers produced by coaxial electrospinning. *Mater Sci Appl*. 2015;6(02):189–199. doi:10.4236/msa.2015.62022
41. Wang M, Zhou Y, Shi D, et al. Cold atmospheric plasma (CAP)-modified and bioactive protein-loaded core-shell nanofibers for bone tissue engineering applications. *Biomater Sci*. 2019;7(6):2430–2439. doi:10.1039/c8bm01284a
42. Liu C, Wang C, Zhao Q, et al. Incorporation and release of dual growth factors for nerve tissue engineering using nanofibrous bicomponent scaffolds. *Biomed Mater*. 2018;13(4):044107. doi:10.1088/1748-605X/aab693
43. Augustine R, Hasan A, Yadu Nath VK, et al. Electrospun polyvinyl alcohol membranes incorporated with green synthesized silver nanoparticles for wound dressing applications. *J Mater Sci Mater Med*. 2018;29(11):205–212. doi:10.1007/s10856-018-6169-7
44. Abdelwahab MA, Flynn A, Chiou BS, Imam S, Orts W, Chiellini E. Thermal, mechanical and morphological characterization of plasticized PLA-PHB blends. *Polym Degrad Stab*. 2012;97(9):1822–1828. doi:10.1016/j.polymdegradstab.2012.05.036
45. Chen B-K, Shih -C-C, Chen AF. Ductile PLA nanocomposites with improved thermal stability. *Compos Part A Appl Sci Manuf*. 2012;43(12):2289–2295. doi:10.1016/J.COMPOSITESA.2012.08.007
46. Hodge RM, Edward GH, Simon GP. Water absorption and states of water in semicrystalline poly(vinyl alcohol) films. *Polymer (Guildf)*. 1996;37(8):1371–1376. doi:10.1016/0032-3861(96)81134-7
47. Firouzi A, Del Gaudio C, Lamastra FR, Montesperelli G, Bianco A. Electrospun polymeric coatings on aluminum alloy as a straightforward approach for corrosion protection. *J Appl Polym Sci*. 2015;132(2). doi:10.1002/app.41250
48. Golafshan N, Rezahasani R, Tarkesh Esfahani M, Kharaziha M, Khorasani SN. Nanohybrid hydrogels of laponite: PVA-alginate as a potential wound healing material. *Carbohydr Polym*. 2017;176:392–401. doi:10.1016/j.carbpol.2017.08.070
49. Naseri N, Algan C, Jacobs V, John M, Oksman K, Mathew AP. Electrospun chitosan-based nanocomposite mats reinforced with chitin nanocrystals for wound dressing. *Carbohydr Polym*. 2014;109:7–15. doi:10.1016/j.carbpol.2014.03.031
50. Augustine R, Kalarikkal N, Thomas S. An in vitro method for the determination of microbial barrier property (MBP) of porous polymeric membranes for skin substitute and wound dressing applications. *Tissue Eng Regen Med*. 2015;12(1):12–19. doi:10.1007/s13770-014-0032-9
51. Shalumon KT, Anjana J, Mony U, Jayakumar R, Chen J-P. Process study, development and degradation behavior of different size scale electrospun poly(caprolactone) and poly(lactic acid) fibers. *J Polym Res*. 2018;25(3):82. doi:10.1007/s10965-018-1475-9
52. Kim SJ, Tatman PD, Song DH, Gee AO, Kim DH, Kim SJ. Nanotopographic cues and stiffness control of tendon-derived stem cells from diverse conditions. *Int J Nanomedicine*. 2018;13:7217–7227. doi:10.2147/IJN.S181743
53. Jiao A, Moerk CT, Penland N, et al. Regulation of skeletal myotube formation and alignment by nanotopographically controlled cell-secreted extracellular matrix. *J Biomed Mater Res A*. 2018;106(6):1543–1551. doi:10.1002/jbm.a.36351
54. Zhao X, Luo J, Fang C, Xiong J. Investigation of polylactide/poly(ϵ -caprolactone)/multi-walled carbon nanotubes electrospun nanofibers with surface texture. *RSC Adv*. 2015;5(120):99179–99187. doi:10.1039/c5ra14301b
55. Sill TJ, von Recum HA. Electrospinning: applications in drug delivery and tissue engineering. *Biomaterials*. 2008;29(13):1989–2006. doi:10.1016/j.biomaterials.2008.01.011
56. Liu Y, Geever LM, Kennedy JE, Higginbotham CL, Cahill PA, McGuinness GB. Thermal behavior and mechanical properties of physically crosslinked PVA/gelatin hydrogels. *J Mech Behav Biomed Mater*. 2010;3(2):203–209. doi:10.1016/J.JMBBM.2009.07.001
57. White RJ, Cutting KF. Interventions to avoid maceration of the skin and wound bed. *Br J Nurs*. 2003;12(20):1186–1201. doi:10.12968/bjon.2003.12.20.11841
58. Moura LIF, Dias AMA, Carvalho E, de Sousa HC. Recent advances on the development of wound dressings for diabetic foot ulcer treatment—A review. *Acta Biomater*. 2013;9(7):7093–7114. doi:10.1016/J.ACTBIO.2013.03.033

59. Hassan A, Niazi MBK, Hussain A, Farrukh S, Ahmad T. Development of anti-bacterial PVA/starch based hydrogel membrane for wound dressing. *J Polym Environ*. 2018;26(1):235–243. doi:10.1007/s10924-017-0944-2
60. Porfyrus A, Vasilakos S, Zotiadis C, et al. Accelerated ageing and hydrolytic stabilization of poly(lactic acid) (PLA) under humidity and temperature conditioning. *Polym Test*. 2018;68:315–332. doi:10.1016/J.POLYMERTESTING.2018.04.018
61. Kokabi M, Sirousazar M, Hassan ZM. PVA-clay nanocomposite hydrogels for wound dressing. *Eur Polym J*. 2007;43(3):773–781. doi:10.1016/j.eurpolymj.2006.11.030
62. Li H, Yang J, Hu X, Liang J, Fan Y, Zhang X. Superabsorbent polysaccharide hydrogels based on pullulan derivate as antibacterial release wound dressing. *J Biomed Mater Res A*. 2011;98 A(1):31–39. doi:10.1002/jbm.a.33045
63. Dumville JC, Deshpande S, O'Meara S, Speak K. Hydrocolloid dressings for healing diabetic foot ulcers. *Cochrane Database Syst Rev*. 2013;2013(8):CD009099. doi:10.1002/14651858.CD009099.pub3
64. Wilson CJ, Clegg RE, Leavesley DI, Percy MJ. Mediation of bio-material–cell interactions by adsorbed proteins: a review. *Tissue Eng*. 2005;11(1–2):1–18. doi:10.1089/ten.2005.11.1
65. Miller DR, Hilton JR, Harding KG, Beuker B, Williams DT. Wound dressings in diabetic foot disease. *Clin Infect Dis*. 2004;39 (Supplement 2):S100–S103. doi:10.1086/383270
66. Edwards J, Stapley S. Debridement of diabetic foot ulcers. *Cochrane Database Syst Rev*. 2010;CD003556. doi:10.1002/14651858.cd003556.pub2
67. Ruszcak Z. Effect of collagen matrices on dermal wound healing. *Adv Drug Deliv Rev*. 2003;55(12):1595–1611. doi:10.1016/J.ADDR.2003.08.003
68. Sakai N, Nakamura M, Lipson KE, et al. Inhibition of CTGF ameliorates peritoneal fibrosis through suppression of fibroblast and myofibroblast accumulation and angiogenesis. *Sci Rep*. 2017;7 (1):5392. doi:10.1038/s41598-017-05624-2
69. Wahab N, Cox D, Witherden A, Mason RM. Connective tissue growth factor (CTGF) promotes activated mesangial cell survival via up-regulation of mitogen-activated protein kinase phosphatase-1 (MKP-1). *Biochem J*. 2007;406(1):131–138. doi:10.1042/bj20061817
70. Fan WH, Pech M, MJ K. Connective tissue growth factor (CTGF) stimulates vascular smooth muscle cell growth and migration in vitro. *Eur J Cell Biol*. 2000;79(12):915–923. doi:10.1078/0171-9335-00122
71. Crean JKG, Finlay D, Murphy M, et al. The role of p42/44 MAPK and protein kinase B in connective tissue growth factor induced extracellular matrix protein production, cell migration, and actin cytoskeletal rearrangement in human mesangial cells. *J Biol Chem*. 2002;277(46):44187–44194. doi:10.1074/jbc.M203715200
72. Livshits G, Kobiela A, Fuchs E. Governing epidermal homeostasis by coupling cell-cell adhesion to integrin and growth factor signaling, proliferation, and apoptosis. *Proc Natl Acad Sci*. 2012;109(13):4886–4891. doi:10.1073/pnas.1202120109
73. Nikitorowicz-Buniak J, Denton CP, Abraham D, Stratton R, Feghali-Bostwick C. Partially evoked epithelial-mesenchymal transition (EMT) is associated with increased TGFβ signaling within lesional scleroderma skin. *PLoS One*. 2015;10(7):e0134092. doi:10.1371/journal.pone.0134092
74. Guo S, Dipietro LA. Factors affecting wound healing. *J Dent Res*. 2010;89(3):219–229. doi:10.1177/0022034509359125
75. Shimo T, Nakanishi T, Kimura Y, et al. Inhibition of endogenous expression of connective tissue growth factor by its antisense oligonucleotide and antisense RNA suppresses proliferation and migration of vascular endothelial cells. *J Biochem*. 1998;124(1):130–140. doi:10.1093/oxfordjournals.jbchem.a022071
76. Nakanishi T, Kuboki T, Tezuka K, et al. Connective tissue growth factor induces the proliferation, migration, and tube formation of vascular endothelial cells in vitro, and angiogenesis in vivo. *J Biochem*. 2012;126 (1):137–145. doi:10.1093/oxfordjournals.jbchem.a022414

International Journal of Nanomedicine

Dovepress

Publish your work in this journal

The International Journal of Nanomedicine is an international, peer-reviewed journal focusing on the application of nanotechnology in diagnostics, therapeutics, and drug delivery systems throughout the biomedical field. This journal is indexed on PubMed Central, MedLine, CAS, SciSearch®, Current Contents®/Clinical Medicine,

Journal Citation Reports/Science Edition, EMBase, Scopus and the Elsevier Bibliographic databases. The manuscript management system is completely online and includes a very quick and fair peer-review system, which is all easy to use. Visit <http://www.dovepress.com/testimonials.php> to read real quotes from published authors.

Submit your manuscript here: <https://www.dovepress.com/international-journal-of-nanomedicine-journal>